

First evidence for di erent freeze-out conditions for kaons and antikaons observed in heavy-ion collisions

A . Forster^b, F . Uhlig^b, I . Bottcher^d, M . D ebowski^{f,g}, F . D ohrm ann^f,
 E . G rosse^{f,g}, P . K oczon^a, B . K ohlm eyer^d, F . Laue^a, M . M enzel^d,
 L . Naumann^f, H . O eschler^b, W . Scheinast^f, E . Schwab^a, P . Senger^a,
 Y . Shin^c, H . Strobel^c, C . Sturm^{b,a}, G . Surowka^{a,e}, A . W agner^f, W . W alus^e

KaoS Collaboration

^a Gesellschaft für Schwerionenforschung, D-64220 Darmstadt, Germany

^b Technische Universität Darmstadt, D-64289 Darmstadt, Germany

^c Johann Wolfgang Goethe-Universität, D-60325 Frankfurt am Main, Germany

^d Philipps Universität, D-35037 Marburg, Germany

^e Jagiellonian University, PL-30059 Krakow, Poland

^f Forschungszentrum Rossendorf, D-01314 Dresden, Germany

^g Technische Universität Dresden, D-01062 Dresden, Germany

Present address: Brookhaven National Laboratory, USA

(Dated: December 24, 2018)

Abstract

Differential production cross sections of K^- and K^+ mesons have been measured in Ni+Ni and Au+Au collisions at a beam energy of 1.5 A GeV. The K^- = K^+ ratio is found to be nearly constant as a function of the collision centrality and system size. The spectral slopes and the polarization pattern differ for K^- and K^+ mesons. These observations indicate that K^+ mesons decouple earlier from the reball than K^- mesons.

PACS numbers: PACS 25.75.Dw

Heavy-ion collisions provide the unique possibility to study baryonic matter well above saturation density. The conditions inside the dense reaction zone and the in-medium properties of hadrons can be explored by measuring the particles created in such collisions [1, 2]. In particular, strange mesons produced at beam energies below or close to the NN threshold are well suited for these studies. The yield of K^+ mesons as measured in Au+Au collisions at SIS/GSI [3] constrains the nuclear matter equation-of-state [4]. The pronounced patterns of the elliptic and directed flow of kaons provide evidence for the existence of a repulsive kaon-nucleon in-medium potential [5, 6]. The K^-/K^+ ratio is enhanced in heavy-ion collisions as compared to proton-proton collisions [7, 8]. In order to reproduce the measured yields, transport model calculations have to take into account density-dependent KN potentials corresponding to an in-medium modification of the K^- meson mass [9, 10]. On the other hand, the measured ratios between strange particles can be explained within statistical models without any in-medium modification of the masses. These models reproduce the measured ratios by choosing an appropriate pair of values for the temperature and the baryon chemical potential assuming thereby a simultaneous chemical freeze-out [11].

Quantitative information on the production mechanisms and the properties of strange mesons in dense baryonic matter can be extracted from the phase-space distributions of K^+ and K^- mesons observed in heavy-ion collisions. In central Au+Au collisions at beam energies above 4 A GeV the spectral slopes were found to be similar for K^+ and K^- mesons [12]. The rapidity density distributions of strange mesons from central Au+Au collisions at 10.7 A GeV and Pb+Pb collisions at 158 A GeV were found to be wider for K^- than for K^+ mesons [13, 14]. In both cases, the K^-/K^+ ratio is constant as a function of the collision centrality. At beam energies below the NN thresholds for strangeness production ($NN \rightarrow K^+ N$ at $E = 1.6$ GeV, $NN \rightarrow K^- K^- N N$ at $E = 2.5$ GeV), where in-medium effects are expected to influence the kaon production significantly, a systematic comparison of K^+ and K^- phase-space distributions has not yet been published.

In this Letter we present results of experiments on K^+ and K^- production in Ni+Ni and Au+Au collisions studied at a beam energy of 1.5 A GeV. This is the lowest beam energy where antikaons have been observed so far in collisions between heavy nuclei. We have measured the spectral and angular distributions of strange mesons as function of the collision centrality and have found significant differences between kaons and antikaons.

The experiments were performed with the Kaon Spectrometer (KaoS) at the heavy-

ion synchrotron (SIS) at GSI in Darmstadt [15]. The magnetic spectrometer has a large acceptance in solid angle and in momentum ($\Delta 30 \text{ m sr}$, $p_{\text{max}} = p_{\text{min}}/2$). The particle identification and the trigger are based on separate measurements of momentum and time-of-flight. The trigger suppresses pions and protons by factors of 10^2 and 10^3 , respectively. The background due to spurious tracks and pile-up is removed by trajectory reconstruction based on three large-area multiwire proportional counters. The short distance of $5 - 6.5 \text{ m}$ from target to focalplane minimizes the number of kaon decays in flight. The loss of kaons by decay is determined and accounted for by Monte Carlo simulations using the GEANT code.

In order to reach an energy of 1.5 A GeV for Au beams, an exceptional operation of the GSI accelerator facility was required: The average charge state of the $^{197}\text{Au}^{63+}$ ions is $63+$ at injection into the synchrotron. In order to strip the ions completely and hence to achieve the highest beam energy, the $^{197}\text{Au}^{63+}$ ions were accelerated with the synchrotron up to an energy of 0.3 A GeV , then extracted and passed through a stripping foil which removed all the electrons from the ions. The $^{197}\text{Au}^{79+}$ ions were injected into the Experimental Storage Ring (ESR) where the beam was cooled by electron cooling, then re-injected into the synchrotron and accelerated to 1.5 A GeV . The final intensity of the ^{197}Au beam at the target was about $6 \cdot 10^7$ ions per spill. The entire multi-stage acceleration cycle took about 25 s.

Due to the energy loss in the Au target (thickness 0.5 mm) the average energy of the Au beam is 1.48 A GeV . The energy loss of the Ni ions in the Ni target is negligible. A high-statistics sample of K mesons was recorded at a polar angle of $\text{lab} = 40^\circ$. The data from Au+Au collisions were also taken in shorter runs at $\text{lab} = 32^\circ, 48^\circ, 60^\circ$ and 72° . The laboratory momenta of the K mesons range from 260 to $1100 \text{ MeV}/c$. The centrality of the collision is derived from the multiplicity of charged particles measured in the interval $12^\circ < \text{lab} < 48^\circ$ by a hodoscope consisting of 84 plastic-scintillator modules.

In order to study the centrality dependence we grouped the data measured close to midrapidity ($\text{lab} = 40^\circ$) into five centrality bins both for Ni+Ni and Au+Au collisions. The most central collisions correspond to 5% of the total reaction cross-section R , the subsequent centrality bins correspond to 15%, 15% and 25% of R . The most peripheral collisions correspond to 40% of R . The total reaction cross-section has been derived from a measurement with a minimum bias trigger and was found to be $\text{R} = 6.0 \pm 0.5 \text{ barn}$.

for $Au + Au$ and $R = 2.9 \pm 0.3$ barn for $Ni + Ni$ collisions. The corresponding number of participating nucleons A_{part} has been calculated from the measured reaction cross-section fractions using a geometrical model assuming a sharp nuclear surface.

Figure 1 shows the production cross sections for K^+ and K^- mesons measured close to midrapidity as a function of the kinetic energy in the center-of-momentum system for the five centrality bins in $Au + Au$ collisions. The uppermost spectra correspond to the most central reactions. The error bars represent the statistical uncertainties of the kaon and the background events. An overall systematic error of 10% due to efficiency corrections and beam normalization has to be added. The solid lines represent the function $E^{-\frac{3}{2}} = dp^3 = C \cdot E \cdot \exp(-E/T)$ fitted to the data. C is a normalization constant and the exponential describes the energy distribution with T as the inverse slope parameter.

The spectra presented in Fig. 1 exhibit a distinct difference between K^- and K^+ : The slopes of the K^- spectra are steeper than those of the K^+ spectra. The inverse slope parameters T are displayed in the upper panel of Figure 2 as a function of the number of participating nucleons A_{part} . T increases with increasing centrality and is found to be significantly lower for antikaons than for kaons, even for the most central collisions. When interpreting spectral slopes one should keep in mind that they are influenced by both the random and the collective motion of the particles (temperature and flow). The radial-flow contribution to the slope depends on the particle mass and hence cannot cause a difference between the K^+ and the K^- spectra. The temperature contribution to the slope is determined at kinetic freeze-out, i.e. at the time when the particles cease to interact.

The multiplicities of K^+ and K^- mesons from $Ni + Ni$ and $Au + Au$ collisions at $1.5 \text{ A} \cdot \text{GeV}$ differ by about a factor of 50. The inclusive kaon multiplicity is defined for each centrality bin as $M = \frac{N}{A_{part}}$ with N the kaon production cross section and A_{part} the reaction cross-section of the particular event class. Figure 2 presents $M = A_{part}$ for K^+ (second panel) and for K^- (third panel) as a function of A_{part} . Both for K^+ and K^- mesons the multiplicities exhibit a similar rise with A_{part} . Moreover, $M = A_{part}$ is found to be almost identical in $Ni + Ni$ and $Au + Au$ collisions. The $K^- = K^+$ ratio is about 0.02 below $A_{part} = 100$ and decreases slightly to about 0.015 for the most central collisions (Figure 2, lowest panel).

Another observable sensitive to the production mechanism is the polar angle emission pattern. The deviation from isotropy of the K^+ and the K^- emission can be studied by the ratio $\frac{_{\text{inv}}(E_{CM}; \theta_{CM})}{_{\text{inv}}(E_{CM}; 90^\circ)}$ as a function of $\cos(\theta_{CM})$. Here, $_{\text{inv}}(E_{CM}; \theta_{CM})$ is

the invariant kaon production cross-section measured at the polar angle $\cos(\theta_{CM})$ in the center-of-momentum frame and $\sigma_{inv}(E_{CM}; 90^\circ)$ is the one measured at $\theta_{CM} = 90^\circ$. Due to limited statistics we considered only Au+Au collisions grouped into two centrality bins: near-central (impact parameter $b < 6 \text{ fm}$) and non-central collisions ($b > 6 \text{ fm}$). Figure 3 displays the anisotropy ratio for K^+ (upper panel) and K^- (lower panel) and for near-central (right) and non-central collisions (left). For an isotropic distribution this ratio would be constant and identical to 1.

The solid lines in Fig. 3 represent the function $1 + a_2 \cos^2(\theta_{CM})$ which is fitted to the experimental distributions with the values of a_2 given in the figure. In near-central collisions the K^- mesons exhibit an isotropic emission pattern whereas the emission of K^+ mesons is forward-backward peaked. The angular distributions observed for K^+ and K^- in Ni+Ni collisions at 1.93 A GeV are similar to the ones presented in Fig. 3 [16]. The measured emission patterns indicate that the antikaons – in contrast to the kaons – have lost the memory of the beam direction for central heavy-ion collisions.

In the following we compare our data to the results of theoretical calculations. Statistical models using a canonical formulation of strangeness conservation predict a constant $K^- = K^+$ ratio as a function of system size for heavy-ion collisions at SIS beam energies [11, 20]. The result of such a calculation is shown in the lowest panel of Figure 2 as a dashed line [11]. In this case a baryochemical potential of $\mu = 770 \text{ MeV}$ and a chemical freeze-out temperature of $T = 63 \text{ MeV}$ was assumed. Measured inverse slope parameters refer to thermal freeze-out and are substantially larger: $T(K^+) = 103 \pm 6 \text{ MeV}$ and $T(K^-) = 93 \pm 6 \text{ MeV}$ for near-central Ni+Ni collisions, and $T(K^+) = 116 \pm 7 \text{ MeV}$ and $T(K^-) = 90 \pm 8 \text{ MeV}$ for near-central Au+Au collisions (corresponding to the average value of the two most central bins in Figure 2, upper panel).

The observation of different spectral slopes or mean energy for K^+ and K^- mesons is at variance with a scenario in which both kaons and antikaons have the same flow velocity and thermal energy at chemical freeze-out. In consequence, the statistical model does not offer a consistent explanation for both the yields and spectral slopes of K^+ and K^- mesons. The difference in spectral slopes rather indicates that K^+ and K^- mesons decouple from the reball sequentially due to their very different KN inelastic cross sections.

Microscopic transport models predict that the kaons and the hyperons are produced via processes like $N N \rightarrow K^+ Y N$ or $N \rightarrow K^+ Y$ with $Y = \pi, \eta$; in the early phase of a heavy-

ion collision [4, 9, 17]. The K^+ mesons leave the reaction volume with little rescattering because of their long mean free path (they contain an anti-s quark and hence cannot be absorbed in hadronic matter consisting almost entirely of u and d quarks). Therefore, the K^+ mesons probe the early, dense and hot phase of the collision and have been used to obtain information on the nuclear equation-of-state [3, 4]. Moreover, transport model calculations have to assume a repulsive in-medium $K^+ N$ potential in order to reproduce both the K^+ yields and the anisotropic azimuthal emission pattern [4].

The K^- mesons can hardly be produced in direct $N N$ collisions at a beam energy of 1.5 A GeV, even when taking into account Fermi motion. According to transport calculations the production of antikaons proceeds predominantly via strangeness-exchange reactions $Y^- + K^- N \rightarrow K^- N$ [9, 18, 19]. The mean free path of the K^- mesons is about 1.5 fm in nuclear matter due to absorption via reactions like $K^- N \rightarrow Y^- + K^-$. However, via the inverse reaction ($Y^- + K^- N \rightarrow K^- + K^- N$) the antikaons may reappear again thus propagating to the surface of the reball. Consequently, the yields of K^+ and K^- mesons are both related to the hyperon yield. With the strangeness-exchange reactions happening continuously during the expansion of the reball, i.e. at decreasing density and temperature, the influence of in-medium properties on the final K^- yield might be reduced. Indeed, transport model calculations claim that the observed K^- mesons in average are produced later than the K^+ mesons [19]. Hence the spectral slope of antikaons is steeper than the one of kaons. Furthermore, the emission pattern of K^- mesons is nearly isotropic due to multiple collisions. These features are observed both in the experiment and in microscopic transport calculations.

The various transport calculations do not yet provide a consistent picture concerning the in-medium properties of antikaons. Recent QMD model calculations predict a rather weak sensitivity of the K^- yield on the $K^- N$ potential [19]. The calculations result in a $K^- = K^+$ ratio which systematically underestimates the experimental data (see the hatched area in the lowest panel of Figure 2) [19]. This result is based on the assumption of in-medium K^+ and K^- masses. A very similar result is obtained for free masses. On the other hand, BUU calculations need to take into account an attractive in-medium $K^- N$ potential in order to explain the K^- yields [9, 10]. Predictions of a BUU model calculation [10] for the $K^- = K^+$ ratio as a function of transverse mass for near-central Au+Au collisions at 1.5 A GeV are shown in Figure 4 together with our experimental results. A similar result was found for $N + N$ collisions at 1.93 A GeV [22]. As demonstrated in Figure 4 the calculations assuming

free K meson masses (dashed line) and in-medium masses (solid line) clearly disagree. In this case the differences in spectral slope are caused by the opposite mean-field potentials of kaons and antikaons. However, both the QMD [19] and the BUU model [10] use a rather simple parametrization of the effective mass of K^+ and K^- mesons in nuclear matter. New theoretical concepts are required to improve the interpretation of experimental data. This is expected from the next generation of transport calculations which will have to take into account off-shell effects like in-medium spectral functions and in-medium cross sections [23].

In summary, we have presented differential cross sections and phase-space distributions of kaons and antikaons produced in heavy-ion collisions at $1.5 \text{ A} \cdot \text{GeV}$. We observed the following features: (i) The $K^- = K^+$ yield ratio is quite independent of A_{part} both for $N + N$ and $Au + Au$ collisions, (ii) in near-central collisions K^- mesons are emitted almost isotropically whereas K^+ mesons exhibit a forward-backward enhanced emission pattern, and (iii) the inverse slope parameters are significantly smaller for K^- than for K^+ mesons even for the most central $Au + Au$ collisions. These findings indicate that (i) the production mechanisms of K^+ and K^- mesons are correlated by strangeness-exchange reactions, (ii) K^- mesons undergo many collisions before leaving the reball and, as a consequence, (iii) K^- and K^+ mesons experience different freeze-out conditions.

[1] J. Aichelin and C. M. Ko, *Phys. Rev. Lett.* 55 (1985) 2661.

[2] G. Q. Li, C. H. Lee and G. E. Brown, *Phys. Rev. Lett.* 79 (1997) 5214.

[3] C. Sturm et al., *Phys. Rev. Lett.* 86 (2001) 39.

[4] C. Fuchs et al., *Phys. Rev. Lett.* 86 (2001) 1974.

[5] Y. Shin et al., *Phys. Rev. Lett.* 81 (1998) 1576.

[6] P. Crochet et al., *Phys. Lett. B* 486 (2000) 6.

[7] R. Barth et al., *Phys. Rev. Lett.* 78 (1997) 4007.

[8] F. Laue, C. Sturm et al., *Phys. Rev. Lett.* 82 (1999) 1640.

[9] W. Cassing and E. Bratkovskaya, *Phys. Rep.* 308 (1999) 65.

[10] G. Q. Li and G. E. Brown, *Phys. Rev. C* 58 (1998) 1698.

[11] J. Cleymans, H. Oeschler and K. Redlich, *Phys. Rev. C* 59 (1999) 1663 and *Phys. Lett. B* 485 (2000) 27.

- [12] L. Ahle et al., *Phys. Rev. C* 58 (1998) 3523.
- [13] N. Herrmann et al., *Ann. Rev. Nucl. Part. Sci.* 49 (1999) 581.
- [14] J. Bachler et al., *Nucl. Phys. A* 661 (1999) 45c.
- [15] P. Senger et al., *Nucl. Instr. Meth. A* 327 (1993) 393.
- [16] M. Münze et al., *Phys. Lett. B* 495 (2000) 26.
- [17] J. Achelin, *Phys. Rep.* 202 (1991) 233.
- [18] C.M. Ko, *Phys. Lett. B* 138 (1984) 361.
- [19] C. Hartnack, H. Oeschler and J. Achelin, *Phys. Rev. Lett.* 90 (2003) 102302 (and private communication)
- [20] G.E. Brown, M. Rho and C. Song, *Nucl. Phys. A* 698 (2002) 483c.
- [21] N. Herrmann, J.P. Wessels and T.W. Jeonold, *Ann. Rev. Nucl. Part. Sci.* 49 (1999) 581.
- [22] K. Wisniewski et al., *Eur. Phys. Jour. A* 9 (2000) 515.
- [23] M. Lutz, *Phys. Lett. B* 426 (1998) 12.

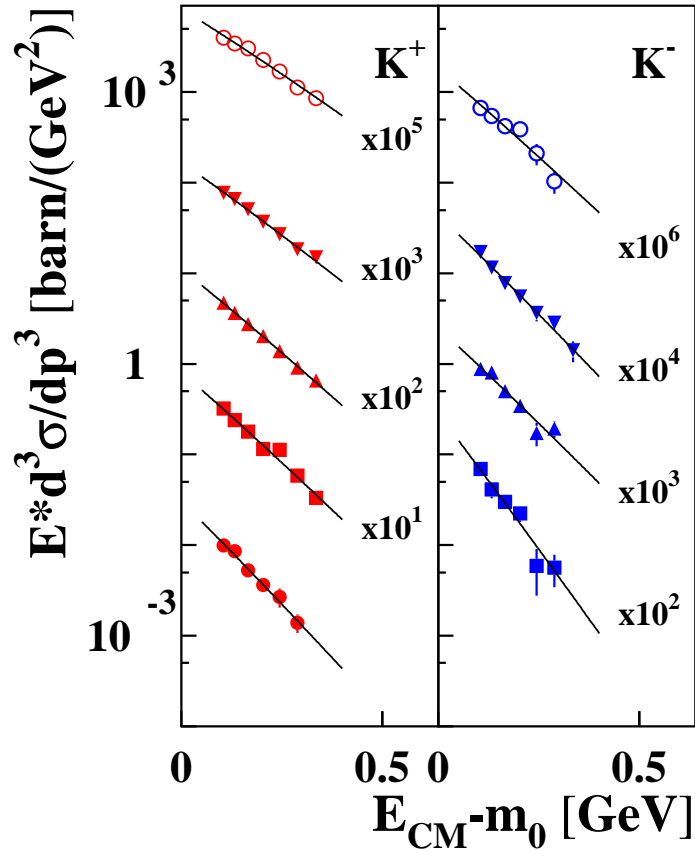


FIG. 1: Differential production cross-sections for K^+ (left) and for K^- mesons (right) from $Au+Au$ collisions at $1.5 A$ GeV for different centrality bins as a function of the kinetic energy in the cm. system. The data were measured at an laboratory angle of $_{lab} = 40^\circ$ which covers midrapidity. The spectra correspond to the following centrality bins (from top to bottom with decreasing centrality): 5%, 15%, 15% and 25% of the reaction cross-section $_{R}$. The lowest K^+ spectrum corresponds to the most peripheral collisions (40% of $_{R}$).

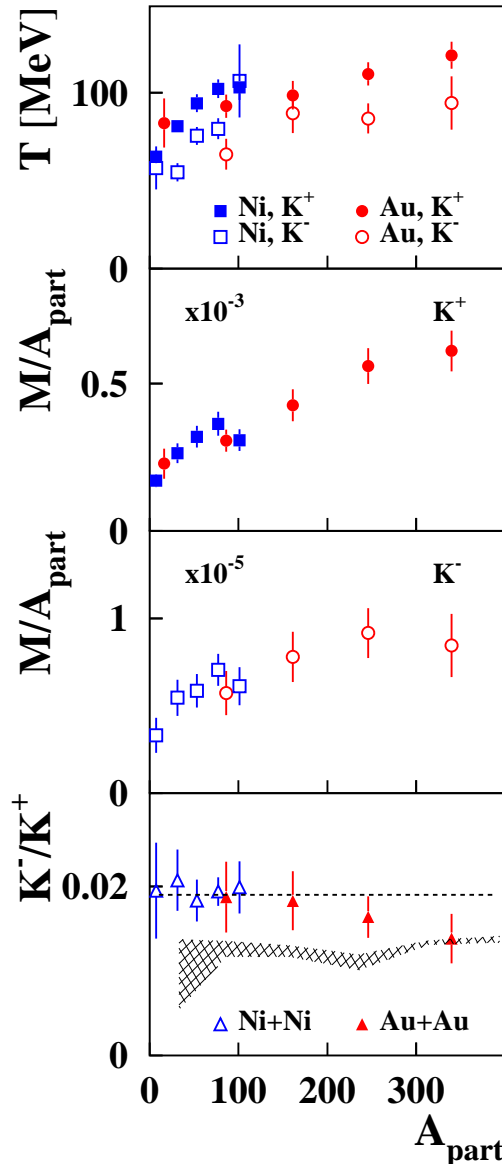


FIG . 2: First panel: Inverse spectral slope parameters of K^+ (full symbols) and of K^- mesons (open symbols) produced in Ni+Ni (squares) and Au+Au collisions (circles) at 1.5 A GeV as a function of the number of participating nucleons. Second and third panel: Multiplicity per number of participating nucleons A_{part} of K^+ and of K^- as a function of A_{part} both for Ni+Ni (squares) and for Au+Au (circles) at a beam energy of 1.5 A GeV . The data were taken at a laboratory angle of $\theta_{\text{lab}} = 40^\circ$. Lowest panel: The ratio of the K^- to K^+ multiplicities as a function of A_{part} . The dashed line represents the result of a statistical model calculation [11]. The cross-hatched area corresponds to the results of a QMD transport model calculation for in-medium masses of K^- mesons [19].

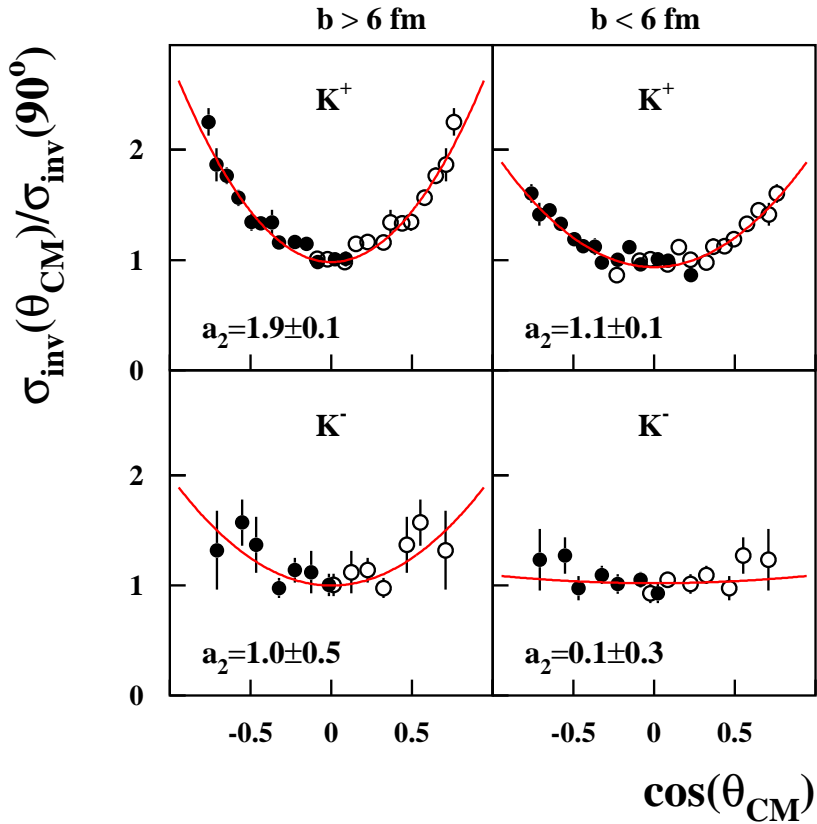


FIG . 3: Polar angle distributions of K^+ (upper panel) and of K^- mesons (lower panel) produced in peripheral (left) and near-central (right) $Au + Au$ collisions at 1.5 A GeV . Full data points are measured and mirrored at $\cos(\theta_{CM}) = 0$ (open points). The lines correspond to the function $1 + a_2 \cos^2(\theta_{CM})$ fitted to the data (see text). The resulting values for a_2 are indicated.

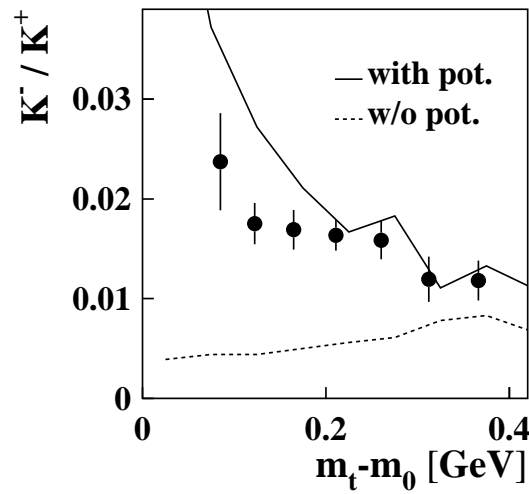


FIG . 4: K^- to K^+ ratio as a function of the transverse mass for near-central ($b < 5$ fm) Au+Au collisions at 1.5 A GeV around midrapidity. The curves represent the predictions of a transport model calculation (BUU) including in-medium potentials (solid line) and for free K meson masses (dashed line). The data (full dots) were taken at $v_{lab} = 40$